

Serveur Académique Lausannois SERVAL serval.unil.ch

Author Manuscript

Faculty of Biology and Medicine Publication

This paper has been peer-reviewed but does not include the final publisher proof-corrections or journal pagination.

Published in final edited form as:

Title: Colon-specific deletion of epithelial sodium channel causes sodium loss and aldosterone resistance.

Authors: Malsure S, Wang Q, Charles RP, Sergi C, Perrier R, Christensen BM, Maillard M, Rossier BC, Hummler E

Journal: Journal of the American Society of Nephrology : JASN

Year: 2014 Jul

Volume: 25

Issue: 7

Pages: 1453-64

DOI: 10.1681/ASN.2013090936

In the absence of a copyright statement, users should assume that standard copyright protection applies, unless the article contains an explicit statement to the contrary. In case of doubt, contact the journal publisher to verify the copyright status of an article.

Colon-specific deletion of α ENaC causes sodium loss and aldosterone resistance

Sumedha Malsure¹, Qing Wang^{2,3}, Roch-Philippe Charles^{1,4}, Chloe Sergi¹, Romain Perrier¹, Birgitte Mønster Christensen^{1,5}, Marc Maillard², Bernard C. Rossier¹, Edith Hummler^{1}.*

¹Department of Pharmacology and Toxicology, University of Lausanne, Lausanne, Switzerland

²Service of Nephrology, University Hospital of Lausanne (CHUV), Lausanne, Switzerland

³Division of Physiology, Department of Medicine, University of Fribourg, Switzerland

⁴Present address: Institute of Biochemistry and Molecular Medicine, University of Bern, Bern, Switzerland

⁵Present address: Department of Biomedicine, Aarhus University, Aarhus, Denmark

Short title: ENaC and CAP1 get limiting on low salt

Keywords: serine protease, *Prss8*, sodium transport, *Scnn1a*, sodium and potassium balance, colonic superficial cells

* Correspondence to:

Edith Hummler, Department of Pharmacology and Toxicology, University of Lausanne, Rue du Bugnon 27, CH-1005, Lausanne, Switzerland; phone: +41-21-6925357, fax: +41-21-

6925355, e-mail: Edith.Hummler@unil.ch

ABSTRACT

The epithelial sodium channel ENaC plays a critical role in the control of sodium and potassium balance in the kidney. In this study, we investigated the importance of ENaC and its positive regulator channel-activating protease 1 (CAP1/*Prss8*) in colon. Mice lacking the α ENaC subunit (*Scnn1a*^{KO} mice) in colonic superficial cells were viable and did not show any fetal or perinatal lethality. Under regular or low salt diet, the amiloride-sensitive rectal potential difference (ΔPD_{amil}) was drastically decreased and its circadian rhythm blunted. Under regular salt or high salt diets or under potassium loading, plasma and urinary sodium and potassium were not significantly changed. However, upon low salt diet, the *Scnn1a*^{KO} mice lost significant amounts of sodium in their feces, accompanied by very high plasma aldosterone and increased urinary sodium retention. Mice lacking the CAP1/*Prss8* (*Prss8*^{KO}) in colonic superficial cells were viable and did not show any fetal or perinatal lethality. Upon regular salt and high salt diets, however, *Prss8*^{KO} mice exhibited a significantly reduced ΔPD_{amil} in the afternoon, but their circadian rhythm was maintained. Upon low salt diet, sodium loss through feces was accompanied by higher plasma aldosterone levels. Thus, we identified the channel-activating protease CAP1/*Prss8* as an important *in vivo* regulator of ENaC in colon. We conclude that, under salt restriction, the absence of ENaC in colonic surface epithelium was compensated by the activation of the renin-angiotensin-aldosterone (RAAS) system in the kidney. This led to a colon-specific pseudohypoaldosteronism type 1 with mineralocorticoid resistance without evidence of impaired potassium balance.

INTRODUCTION

Sodium and potassium transport across tight epithelia (kidney, colon) is important to keep the body in a constant balance despite large dietary variations. Aldosterone promotes sodium reabsorption as an electrogenic sodium transport via the amiloride-sensitive epithelial sodium channel ENaC¹. Systemic autosomal recessive pseudohypoaldosteronism type 1 (systemic PHA-1) is caused by ENaC mutations and characterized by a severe salt-losing syndrome paralleled with hypotension, hyperkalemia, metabolic acidosis and high plasma aldosterone levels². Liddle's syndrome is due to mutations within the PY-domain of the β or γ ENaC subunits and results in severe salt-sensitive hypertension with renal salt-retention, alkalosis and low plasma aldosterone levels³.

ENaC was originally identified in rat colon from animals challenged with low salt diet and is made of three homologous subunits α , β and γ ^{4,5}. The murine constitutive knockout of each subunit is postnatally lethal⁶⁻⁸. In absence of α ENaC, the β and γ subunits are not transported to the membrane and no amiloride-sensitive sodium current is measured *in vitro* or *ex vivo*^{6,9}.

Along the intestine, sodium absorption occurs through electroneutral sodium transport via the sodium/hydrogen exchanger (NHE) rather than electrogenic absorption via ENaC that is limited to surface epithelial cells of distal colon and rectum^{10, 11}. Following proctocolectomy, ENaC starts to be expressed in the distal part of the small intestine, i.e., the ileum, thereby unveiling the importance of an electrogenic amiloride-sensitive transport for the reabsorption of salt and water in the intestine¹². Thereby, aldosterone stimulates β and γ ENaC mRNA transcript expression in rat distal colon¹³⁻¹⁵. If dietary sodium intake is low and plasma aldosterone levels are high, the distal colon can efficiently absorb dietary sodium against a large concentration gradient^{11, 16}. Enhanced ENaC expression in colon thus contributes to sodium retention observed in mice with Liddle's syndrome^{17, 18} along with

increased responsiveness to aldosterone¹⁹. On the other side, down-regulation of ENaC with reduction in sodium reabsorption in colon may contribute to diarrhea associated with inflammatory bowel disease^{20,21}.

The membrane bound serine protease CAP1/*Prss8*, also known as prostaticin activates ENaC by rapidly increasing the open probability²²⁻²⁵. CAP1/*Prss8* is co-expressed with ENaC in many salt-absorbing tight epithelia, such as distal colon, urinary bladder, and airways^{23,24}. First *in vivo* evidence that CAP1/*Prss8* is an important and physiologically relevant activator of ENaC came from the study of mice lacking CAP1/*Prss8* in the alveolar epithelium unveiling a crucial role for lung fluid balance²⁶. In the colon however, the physiological role of this membrane-serine protease was hitherto unknown and it was unclear whether CAP1/*Prss8* was implicated in regulating colonic ENaC activity.

In the present study, we thus addressed whether suppression of colonic ENaC activity affected sodium and/or potassium balance, and/or what are the compensatory mechanisms that lead to increased renal sodium reabsorption. And finally, we unveiled the role of the positive ENaC activator CAP1/*Prss8* in colon. We specifically deleted either α ENaC/*Scnn1a* or CAP1/*Prss8* in the colonic surface epithelium and determined *in vivo* the electrogenic sodium transport to correlate plasma electrolytes with fecal sodium loss and plasma aldosterone concentrations.

RESULTS

Intestine-specific α ENaC-deficient mice are viable and exhibit normal colon histology

To ablate α ENaC expression in colonic superficial cells, we mated *Scnn1a*^{+/-}; *villin::Cre*^{tg/0} mice with mice harboring two floxed α ENaC alleles (*Scnn1a*^{loxlox}; **Fig. 1A**). Analysis of a total of 252 offspring at weaning showed no deviation from the expected Mendelian distribution (*Scnn1a*^{Lox}, n= 60; *Scnn1a*^{Het}, n= 68; *Scnn1a*^{Hetc}, n= 70; *Scnn1a*^{KO}, n= 54). Adult *Scnn1a*^{KO} mice were viable, showed no postnatal mortality, and were indistinguishable in appearance, growth and body weight (**Table 1**). In the *Scnn1a*^{KO} mice, colonic superficial cells lack near 99 % of *Scnn1a* mRNA transcript expression, while heterozygotes (*Scnn1a*^{Het}) exhibit intermediate (71%) expression levels compared to *Scnn1a*^{Lox} (left panel, $P < 0.05$; **Fig. 1B**). The expressions of β and γ ENaC mRNA transcripts were not significantly higher in *Scnn1a*^{KO} mice (**Fig. 1B**). The successful deletion of *Scnn1a* in scraped colonic superficial cells was further confirmed on the protein expression level (**Fig. 1C and D**). Heterozygotes for the *Scnn1a* allele (*Scnn1a*^{Het} and *Scnn1a*^{Hetc}) showed intermediate expression (70% and 50 % of *Scnn1a*^{Lox}), respectively.

Macroscopically, the morphology of the adult distal colon was not different (**Suppl. Fig.1**). The colon epithelium and mucin-secreting goblet cells appeared normal in knockout mice, without any effect on the number of crypt cells (not shown). The intestine length-to-body weight ratio was not different between the *Scnn1a*^{Lox} (1.97 ± 0.05), *Scnn1a*^{Het} (1.89 ± 0.05) and *Scnn1a*^{KO} (1.83 ± 0.06) groups.

Implication of ENaC in intestinal electrogenic sodium transport and sodium balance

ENaC-mediated sodium transport is electrogenic and generates an amiloride-sensitive transepithelial potential difference (ΔPD_{amil}) that varies upon different salt diets and follows a circadian rhythm²⁷. We measured ΔPD_{amil} , and the switch from HS (**Fig. 2A**) to RS (**Fig. 2B**)

and to LS (**Fig. 2C**) diets induced a progressive increase in plasma aldosterone (**Fig. 3**). Upon HS diet, plasma aldosterone (0.1-0.2 nmol/l) (**Fig. 3**) and baseline ΔPD_{amil} (**Fig. 2A**) were equally low (-5 to -6 mV) between groups (**Fig. 2A**). Upon RS diet, plasma aldosterone increased from 0.7 nmol/l in *Scnn1a*^{Lox} to 1.2 nmol/l in *Scnn1a*^{Het} and to 1 nmol/l in *Scnn1a*^{Hetc} (**Fig. 3**). All mice showed a significant (-10 to -15 mV) increase in ΔPD_{amil} in comparison to the HS diet. The circadian rhythm expressed as (am/pm) cyclicity was readily observed (**Fig. 2A, B**). The highest plasma aldosterone was observed in the *Scnn1a*^{KO} group (2.4 nmol/l) contrasting with the ΔPD_{amil} that remained low (-6 to -8 mV) and without cyclicity (**Fig. 2B, 3**). Upon LS diet, plasma aldosterone increased in all groups to reach high values in the *Scnn1a*^{KO} group (8.5 nmol/l; **Fig. 3**). Despite this drastic increase in plasma aldosterone level, ΔPD_{amil} remained low (-5 to -6 mV) with blunted cyclicity (**Fig. 2C, 3**). In all conditions, a residual amiloride-insensitive negative PD was observed (between -6 and -8 mV) (data not shown). The observed hyperaldosteronism suggested that loss of sodium in the feces could have caused a significant hypovolemia and triggered the activation of the renin-angiotensin-aldosterone system (RAAS). We therefore analyzed total sodium and potassium in the feces, and found that upon regular (RS) and low salt (LS) diet, *Scnn1a*^{KO} mice lost significantly more sodium (RS, $P < 0.05$; LS, $P < 0.001$). This difference was not observed upon high salt diet (**Fig. 4A**). Fecal potassium was not significantly different amongst the groups (**Fig. 4B**). Moreover, wet/ dry ratio of feces was similar in all groups (*Scnn1a*^{KO}: 0.32 ± 0.02 , *Scnn1a*^{Lox}: 0.30 ± 0.02 and *Scnn1a*^{Het}: 0.34 ± 0.02).

The kidney compensated missing ENaC-mediated sodium absorption

Scnn1a^{KO} mice should be able to compensate the fecal sodium loss by an aldosterone-dependent sodium absorption by distal nephron. Hence, mice were followed in metabolic cages and, upon HS, RS and LS diets, food and water intake, feces output, urinary volume,

plasma and urinary sodium and potassium were measured (**Table 1**). Only upon LS diet, cumulative sodium excretion in the *Scnn1a*^{KO} group was significantly diminished as compared to all groups (**Fig. 5A-C**; $P < 0.05$). Cumulative potassium loss was not different even when challenged with high potassium (HK, 5%; **Table. 1**; **Fig. 5D-F**).

CAP1/Prss8 identified as an in-vivo regulator of ENaC in distal colon

To test the role of CAP1/*Prss8* on ENaC in distal colon *in vivo*, intestine-specific CAP1/*Prss8*-deficient mice (*Prss8*^{KO}, *Prss8* ^{Δ /lox}; *villin::Cre*^{tg/0}) were generated (**Fig. 6A**). At weaning, analysis of a total of 219 offspring showed no deviation from the Mendelian distribution (*Prss8*^{Lox}, n= 55; *Prss8*^{Het}, n= 55; *Prss8*^{Hetc}, n= 56; *Prss8*^{KO}, n= 53). In *Prss8*^{KO} mice, colonic superficial cells lacked CAP1/*Prss8* mRNA transcript expression (<1%) while heterozygotes (*Prss8*^{Het}) exhibited intermediate expression levels compared to *Prss8*^{Lox} cells (70%; **Fig. 6B**). The mRNA transcript expression of CAP2/*Tmprss4* and CAP3/*Prss14* was not altered (**Fig. 6B**). The successful deletion of CAP1/*Prss8* in scraped colonic superficial cells was further confirmed on the protein level (**Fig. 6 C-D**).

Prss8^{KO} mice did not differ in body weight, food and water intake, urine or feces output and plasma and urinary sodium and potassium levels (**Table. 2**). Colon histology was normal (**Suppl. Fig. 2A**) without any apparent effect on the number of crypt cells (data not shown). The intestine length-to-body weight ratio was not different between the wild type like (*Prss8*^{Lox}: 2.04 \pm 0.14), heterozygotes (*Prss8*^{Het}: 2.16 \pm 0.13) and knockout (*Prss8*^{KO}: 1.91 \pm 0.1) ($P = 0.4$). When we monitored the intestinal permeability following fluorescein isothiocyanate dextran supply in blood plasma, we found that, besides a slight increase in knockouts, the intestinal barrier function was not significantly increased ($P = 0.09$ to *Prss8*^{Het}, and $P = 0.39$ to *Prss8*^{Lox}; **Suppl. Fig. 2B**). When mRNA expression levels of ENaC subunits were quantified in distal colon and in the kidney, there was not difference amongst the groups with the

exception of β ENaC mRNA transcripts, (KO versus Lox and Het, $P<0.05$; **Suppl. Fig. 3A, B**). Western blot analysis using the anti- α ENaC antibody revealed the full-length 93kDa form and its cleaved 30kDa form (**Suppl. Fig 3C**). The 95kDa full-length β - and γ ENaC including the cleaved 75kDa γ ENaC proteins are equally present in all groups (**Suppl. Fig 3 C-F**). We finally measured ΔPD_{amil} following HS, RS and LS diets that induced a progressive increase in plasma aldosterone levels in all groups (**Fig. 7 A-D**). Upon HS diet, baseline ΔPD_{amil} and plasma aldosterone levels (0.1-0.2 nmol/l) were equally low (-8 to -10 mV) and cyclicality was maintained, although blunted (**Fig. 7A, D**). Upon RS diet, ΔPD_{amil} of $Prss\delta^{Lox}$ and $Prss\delta^{Het}$ mice increased markedly (-15 to -25 mV) with respect to HS diet and (am/pm) cyclicality was readily observed (**Fig. 7A, B**). Despite increased (0.5 nmol/l) plasma aldosterone levels, the cyclicality of the $Prss\delta^{KO}$ group was blunted, mainly due to a significant decrease of ΔPD_{amil} in the afternoon. Upon LS diet, ΔPD_{amil} in $Prss\delta^{KO}$ remained significantly lower with blunted cyclicality, although plasma aldosterone levels reached comparable high and even significant values (**Fig. 7C, D**; $P<0.05$). Interestingly, however, the feces wet/ dry ratio was not altered in the knockout ($Prss\delta^{KO}$: 0.33 ± 0.02 versus controls, $Prss\delta^{Lox}$: 0.31 ± 0.02 and $Prss\delta^{Het}$: 0.37 ± 0.02 ; $P =0.4$), and sodium, but not potassium was significantly lost in feces from the knockouts (**Fig. 7E, F**; $P< 0.05$).

In summary, our data clearly demonstrate that *in vivo* stimulation of the amiloride-sensitive ENaC-mediated sodium transport is dependent on the expression of the membrane-bound serine protease CAP1/*Prss8*, and more strikingly in the afternoon when the RAAS is maximally activated.

DISCUSSION

ENaC-mediated electrogenic sodium transport is limiting for the final absorption of sodium in distal colon and rectum: evidence for colon-specific haploinsufficiency

In the present study, we studied mice with an efficient deletion of α ENaC along the colon and found a strict gene dosage effect at the mRNA transcript and protein expression level (**Fig. 1**). Electrogenic sodium transport in distal colon was mainly mediated by ENaC even if a low but significant electrogenic transport was measured following amiloride application (**Fig. 2**). We cannot exclude some residual ENaC activity due to incomplete recombination even though, upon a high salt (HS) diet, mRNA expression of ENaC subunits should be rather repressed. NHE3 that is sensitive to amiloride is electroneutral and thus undetectable by our PD measurements (**Fig. 2**). Upon RS diet and despite increased plasma aldosterone levels, the ENaC KO mice remained at a low ΔPD_{amil} . Under LS diet, a significant dissociation between the heterozygotes and the floxed (*Scnn1a*^{Lox}) group was observed indicating haploinsufficiency possibly due to upregulation of AT1 receptors, although those mice showed an intact capacity to maintain blood pressure and sodium balance²⁸.

Differential activation of RAAS when lowering salt intake: evidence for colon-specific mineralocorticoid resistance

In our study, we have varied salt intake from HS to RS (19-fold) and from RS to LS diet with an additional 17-fold decrease in salt intake (**Suppl. Fig. 4**). The *Scnn1a*^{KO} mice showed a 14-fold (versus 7-fold in control groups, $P < 0.05$; HS to RS) increased aldosterone response that declined upon switch from RS to LS to a 4-fold ($P < 0.01$; versus 2-fold) induction (**Suppl. Fig. 4**). Absence of ENaC in colon and consequently failure of the colon to absorb sodium against an electrochemical gradient might lead to a colon-specific salt losing syndrome accompanied by high aldosterone response as demonstrated by the clear correlation between

plasma aldosterone (P_{aldo}) levels and ΔPD_{amil} response; the KO mice remained unresponsive whereas the *Scnn1a*^{Lox} mice stayed sensitive to increased P_{aldo} . The response of the heterozygous mice was intermediate ($P < 0.05$; **Suppl. Fig. 4, 5**). We interpreted these data as indicating a colon-specific mineralocorticoid resistance (or decreased aldosterone responsiveness) that led to a colon-specific PHA-1 phenotype. Interestingly, a mirrored image of this phenotype was observed in colon of Liddle mice that harbor a point mutation within the β ENaC subunit leading constitutively to hyperactivity of ENaC and an increased aldosterone responsiveness of the sodium transport in colon^{19, 29}.

Differential effect of colon-specific α ENaC knockouts on sodium and potassium balance

As summarized in **Fig. 8**, upon HS diet, *Scnn1a*^{KO} mice exhibit a sodium balance and the total recovery of urinary and fecal sodium accounts for approximately 85% of sodium intake. From HS to LS diet, we found a progressive fecal sodium loss in *Scnn1a*^{Het/c} and *Scnn1a*^{KO} mice. Under LS, the fecal loss of sodium is compensated by a maximal retention of sodium in the kidney due to high P_{aldo} (**Fig. 4, 8**). The missing sodium might be due to loss into the transcellular fluid compartment that may account for about 6 % along the entire intestine and/or into the skin compartment³⁰. Although systemic PHA-1 is normally also characterized by hyperkalemia, we did not find a shift in the potassium balance in the *Scnn1a*^{KO} mice (**Fig. 4, 5**) that may be explained by a differentially regulated and spatially separation of electrogenic sodium absorption and potassium secretion³¹.

CAP1 regulates colon ENaC activity by blunting its circadian cyclicality

Previous studies have emphasized the importance of CAP1/Prss8 *in vivo*³²⁻³⁵ and its implication in ENaC regulation in alveolar fluid clearance and lung fluid balance²⁶. In colon, we clearly identify CAP1/Prss8 as a protease activating ENaC *in vivo*, since upon RS and LS

diets, ENaC-mediated transport becomes limiting in *Prss8*^{KO} mice (**Fig. 7**). These data are in the same line as recent findings in hairless (*fr*^{CR}) rats and frizzy (*fr/fr*) mice harboring spontaneous mutations of *CAP1/Prss8*³². We do not see an implication of *CAP1/Prss8* in epithelial barrier formation and permeability in colon (**Suppl. Fig. 2**) contrary to mice that specifically lack *CAP1/Prss8* in the epidermis and exhibit a severely impaired epidermal barrier due to defective function of tight junctions³⁴. Interestingly, lack of the serine protease in colon superficial cells is not consistent with a failure to cleave ENaC as the cleaved 75kDa ENaC fragment is well present in *Prss8*^{KO} mice (**Suppl. Fig. 3**). These data is consistent with previous findings, where the 80kDa and the cleaved 70kDa gamma ENaC protein forms were detected, when *CAP1/Prss8* was absent in lung²⁶. This lack of difference in γ cleavage is maybe not too surprising in view of the relative small difference in ΔPD_{amil} between the KO and the controls.

In conclusion, we demonstrated that in colon of mice lacking ENaC and/or *CAP1/Prss8*, amiloride-sensitive sodium transport is drastically diminished. This leads to increased fecal sodium loss, which is accompanied by mineralocorticoid resistance in ENaC-deficient mice. In patients with PHA-1 mutations, this might become pathophysiologically relevant and aggravate sodium loss, in particular upon low dietary salt intake. Since the amount of sodium in the body is the main determinant of extracellular volume, disturbances in sodium balance will lead to clinical situations of volume depletion or overload; the latter will lead to arterial hypertension and heart failure. In CKD, when the ability of the kidneys to excrete sodium decreases, pharmacological inhibition of colonic ENaC may lead to increased intestinal excretion of sodium. This may help to maintain sodium homeostasis in CKD where diuretics have only limited success.

CONCISE METHODS

Intestine-specific CAP1/*Prss8* and α ENaC-deficient mice

Intestine-specific α ENaC (*Scnn1a*) or CAP1/*Prss8* knockout mice were generated by interbreeding *Villin::Cre* transgenic mice (el Marjou et al., 2004) which were heterozygous mutant for the α ENaC⁶ or CAP1/*Prss8*³⁴ knockout allele with mice homozygous for the respective conditional alleles *Scnn1a*^{loxlox36}, or CAP1/*Prss8*^{lox/lox}³⁷. To generate an intestine-specific α ENaC KO, we mated *Scnn1a*^{+/-}; *villin::Cre*^{tg/0} mice with mice harboring two floxed α ENaC alleles (*Scnn1a*^{loxlox}). Age-matched wild type-like *Scnn1a*^{lox/+} (*Scnn1a*^{Lox}), heterozygous mutant, *Scnn1a*^{lox/-} (*Scnn1a*^{Het}), intestine-specific heterozygous mutant, *Scnn1a*^{lox/+}; *villin::Cre*^{tg/0}, (*Scnn1a*^{Hetc}) and intestine-specific α ENaC knockout, *Scnn1a*^{lox/-}; *villin::Cre*^{tg/0}, (*Scnn1a*^{KO}) mice were obtained. To generate intestine-specific CAP1/*Prss8* KO, we mated *Prss8* ^{Δ /+}; *villin::Cre*^{tg/0} mice with mice harboring two floxed CAP1/*Prss8* (*Prss8*^{loxlox}). Age-matched wild type-like CAP1/*Prss8*^{lox/+} (*Prss8*^{Lox}), heterozygous mutant, CAP1/*Prss8*^{lox/ Δ} (*Prss8*^{Het}), intestine-specific heterozygous mutant, CAP1/*Prss8*^{lox/+}; *villin::Cre*^{tg/0}, (*Prss8*^{Hetc}) and intestine-specific CAP1/*Prss8* knockout, CAP1/*Prss8*^{lox/ Δ} ; *villin::Cre*^{tg/0}, (*Prss8*^{KO}) mice were obtained.

All animal work was conducted according to Swiss federal guidelines. All mice were kept in the animal facility under UNIL animal care regulations. They were housed in individual ventilated cages at 23±1 °C with a 12-h light/dark cycle. All animals were supplied with food and water ad libitum. This study has been reviewed and approved by the “Service de la consommation et des affaires vétérinaires” of the Canton of Vaud, Switzerland. If not otherwise indicated, 6-12 weeks old age-matched male and female α ENaC and CAP1/*Prss8* control and experimental (knockout) mice (homozygous for *Ren-1^c*) were fed for at least 3 weeks with regular (RS, 0.17% Na⁺), high-salt (HS, 3.2% Na⁺), or low-salt

(LS, 0.01% Na⁺) diet. All diets were obtained from ssniff Spezialdiäten GmbH, Soest, Germany.

Genotyping

Genotyping by PCR was performed using the following primers: **CAP1/Prss8^{+lox/Δ}**:

Prss8-1 sense, (5'-GCAGTTGTAAGCTGTCATGTG-3');

Prss8-2 sense, (5'-CAGCAGCTGAGGTACCACT-3');

Prss8-3 antisense, (5'-CCAGGAAGCATAGGTAGAAG-3');

αENaC^{+/-}: αENaC^{+/-}-1 antisense, (5'-TTAAGGGTGCACACAGTGACGGC-3');

αENaC^{+/-}-2 antisense, (5'-TTTGTCACGTCCTGCACGACGCG-3');

αENaC^{+/-}-3 sense (5'-AACTCCAGAAGGTCAGCTGGCTC-3');

αENaC^{+lox/Δ}: αENaC^{lox/+}-1 sense (5'-CTCAATCAGAAGGACCCTGG-3');

αENaC^{lox/+}-2 sense (5'-GTCACTGTGTGCACCCTTAA-3');

αENaC^{lox/+}-3 antisense (5'-GCAAAAGATCTTATCCACC-3').

If not otherwise stated, 35 cycles were run, each consisting of 1 min at 94°C, 56°C (58°C for ENaC) and 72°C. The *Villin::Cre* transgene was detected by PCR using the following primers: *Villin-Cre* sense (5'-CCTGGAAAATGCTTCTGTCCG-3'); and

Villin-Cre antisense (5'-CAGGGTGTATAAGCAATCCC-3').

Myogenin-specific primers (sense, 5'-TTACGTCCTCGTGGACAGC-3'); and

antisense (5'-TGGGCTGGGTGTTAGTCTTA-3') were used to control the DNA integrity of each sample.

Quantitative RT-PCR analysis on distal colon and kidney samples

Total RNA was prepared from freshly isolated mouse colon superficial cells and whole kidney using the RNeasy extraction kit (Qiagen, Hilden, Germany). The RNA (1μg/sample) was reverse-transcribed at 37°C for 1h using superscript II RNase H-reverse-transcriptase (Invitrogen, Basel, Switzerland) and oligo-dT(20) primers (Invitrogen). The products were

then diluted ten times before proceeding with the real-time PCR reaction. Real-time PCRs were performed by Taqman[®] PCR with the Applied Biosystems 7500 (Foster City, CA, USA). The primers and probes mix 20X (Mm00504792 m1 for mCAP1 and 4352341E for β -actin) were purchased with the Universal Taqman mix 2X and used according to the manufacturer instructions (Applied Bio systems, Foster City, CA, USA). Quantification of fluorescence was performed with the $\Delta\Delta C_T$ normalized to β -actin. Each measurement was performed in duplicate. Further following primers have been used:

Scnn1a, FOR, 5'-GCACCCTTAATCCTTACAGATACACTG-3' and
REV, 5'-CAAAAAGCGTCTGTTCCGTG-3',

Probe 5'-FAM-AGAGGATCTGGAAGAGCTGGACCGCA-BHQ1-3';

Scnn1b, FOR, 5'-GGGTGCTGGTGGACAAGC-3',
REV, 5'-ATGTGGTCTTGAAACAGGAATG-3',

Probe, 5'-FAM-CAGTCCCTGCACCATGAACGGCT-BHQ1-3';

Scnn1g, FOR, 5'-AACCTTACAGCCAGTGCACAGA-3',
REV, 5'-TTGGAAGCATGAGTAAAGGCAG-3',

Probe, 5'-FAM-AGCGATGTGCCCGTCACAAACATCT-BHQ1-3';

Prss8, FOR, 5'-CCCATCTGCCTCCCTGC-3',
REV, 5'-CCATCCCGTGACAGTACAGTGA-3',

Probe, 5'-FAM CCAATGCCTCCTTTCCCAACGGC-BHQ1-3';

Prss14, FOR, 5'-GAAGCTTTGATGTCGCTCCC-3',
REV, 5'-GGAGGGTGAGAAGGTGCCA-3',

Probe, 5'-FAM- CCACGCTGTGGTGC GGCTG-BHQ-1-3';

Tmprss4, FOR, 5'-AGTAGGCATCGTGAGCTGGG-3',
REV, 5'-GGACGGCAGCGTTACATCTC-3',

Probe, 5'-FAM-ATGGATGCGGCGGCCCAA-BHQ1-3'.

Western blot analysis

Animals (n= 3-4 months old) were kept under a RS diet or LS diet for 2 weeks. Colon and kidney were freshly isolated and snap frozen in liquid nitrogen. Proteins were extracted by homogenization using polytron and by sonication with an IKA sonicator in 8M urea buffer, then incubated 30' on ice and centrifuged for 30' at 4°C at 14000 rpm. The supernatant was taken and centrifuged again for 10' at 4°C at 14000 rpm. The supernatant was used to detect the protein concentration with a BCA protein kit (PIERCE, Rockford, IL, USA). Samples of protein extracts were separated by SDS-PAGE on 10% acrylamide gels, electrically transferred to polyscreen polyvinylidene difluoride (PVDF) transfer membrane (Perkin Elmer, Boston, USA) and subsequently probed for CAP1/*Prss8*, Scnn1a (α ENaC), Scnn1b (β ENaC), Scnn1g (γ ENaC) and β -actin by using primary rabbit antibodies Scnn1a, 1:500³⁸; Scnn1b and Scnn1g, 1:1000³⁹; CAP1, 1:1000⁴⁰; β -actin, 1:1000 (Sigma) and anti-rabbit IgG secondary antibody (1:10000, Amersham Pharmacia Biotech, UK). The signal was developed with ECL+ system (Amersham, HyperfilmTM ECL, Buckinghamshire, UK). Quantification of protein level was obtained using NIH image software.

Histological analysis of proximal and distal colon

Colons were fixed in 4% paraformaldehyde overnight and subjected to paraffin embedding and sectioning (4 μ m sections). These were stained with haematoxylin and eosin and were examined by light microscopy using an Axioplan microscope (Carl Zeiss Microimaging, Inc. Oberkochen/Jena, Germany) and images were acquired with a high sensibility digital color camera (Carl Zeiss Microimaging, Inc.).

Determination of intestine structural and functional parameters

Determination of length-to-body weight. Length of intestine (cm) was individually measured and normalized to its body weight from 3-months-old mice. Results were determined as mean \pm SE.

Feces wet-to-dry weight and electrolyte measurements. Feces samples were collected from age-matched 3 months old control (n=6), heterozygote mutant (n=6) and knockout (n=7) mice that were kept under regular salt diet in metabolic cages for 4 consecutive days. Wet-to-dry weight was determined by determining the wet weight feces samples collected within 24 hours, dried at 80°C for further 24 hours for desiccation and weighed again to calculate the wet-to-dry feces ratio as described ³². Sodium and potassium fecal electrolytes were determined from samples as described ⁴¹. Briefly, the feces were collected over two consecutive days, weighed and resuspended overnight into 0.75N nitric acid at 4°C. After centrifugation an aliquot of supernatant was measured for Na⁺ and K⁺ content with a flame photometer (Instrumentation Laboratory 943 Electrolyte Analyzer, UK).

Intestinal permeability assay. *In vivo* intestinal permeability was determined as described previously ⁴². Briefly, mice were kept under regular salt diet and gavaged with 10 ml/kg of a solution of 22 mg/ml fluorescein isothiocyanate (FITC) - dextran (4 kDa, Sigma, St. Louis, MO, USA) in PBS, pH 7.4. Three hours following gavage, plasma was collected at the end of the experiment, centrifuged at 3000 rpm for 20 min. at 4°C. Following a 1:1 dilution in PBS, the concentration of fluorescein was determined using a 96-plate reader with an excitation wavelength at 485nm and an emission wavelength at 535 nm using serially diluted samples of the tracer as a standard.

Metabolic cage studies. 6-12 weeks old age-matched control and knockout mice were individually placed in metabolic cages (Tecniplast, Buguggiate, Italy) for 5 consecutive days to measure urine and feces output. Food and water intake was daily measured. For the entire

experiment, mice had free access to food and water. During experimental days, urine and feces were collected. Sodium intake was measured as sodium (mmol) intake per day in percentage of total food intake. Sodium output was measured as urinary sodium (mmol) and fecal sodium (mmol) excretion per day in percentage of total food intake.

High-Potassium Diet

Experimental mice and control mice were placed in individual metabolic cages and fed a standard diet for 2 consecutive days (0.95% potassium). This was followed by 2 days on 5% potassium in drinking water (the potassium was added as KCl). During the experiment, the animals had free access to food and water. During experimental days, urine was collected. Blood and urine were collected 2 days after the experiment.

Analyses of urinary electrolytes and blood plasma analysis

Twenty four hour urine samples were collected in metabolic cages. Blood samples were collected at the end of the experiment. Urine and plasma electrolytes were analyzed using an Instrumentation Laboratory 943 Electrolyte Analyzer (UK).

Blood collection for aldosterone measurements

Control and knockout mice (8-12 weeks old) were kept in standard cages with free access to food and water and fed with RS, LS or HS diets for 12 consecutive days. At the end of the experiment, blood samples were collected. Plasma aldosterone levels were measured according to standard procedures using a radioimmunoassay (RIA) (Coat-A-Count RIA kit, Siemens Medical Solutions Diagnostics, Ballerup, Denmark)⁴³. Samples with values > 1200 pg/ml were further diluted using a serum pool with a low aldosterone concentration (<50 pg/ml). Aldosterone concentration is indicated as nmol/l.

Amiloride-sensitive rectal transepithelial potential difference measurements

Mice were fed a low salt (LS) and high salt diet (HS) during 3 weeks. Amiloride-sensitive transepithelial rectal PD measurements were performed as previously described^{27,32}. Briefly, rectal potential difference (PD) and amiloride-sensitive rectal PD were measured in the morning (10 am to noon) and in the afternoon (4 pm to 6 pm) on two days of the same week. The rectal PD was monitored continuously by a VCC600 electrometer (Physiologic instruments, San Diego, CA, USA) connected to a chart recorder. After stabilization of rectal PD (approx. 1 min), 0.05 ml saline solution was injected through the first barrel as a control manoeuvre and the PD was recorded for another 30 seconds. A similar volume of saline solution containing 25 $\mu\text{mol/l}$ amiloride was injected through the second barrel of the pipette and the PD was recorded for 1 min. The potential difference was recorded before and after the addition of amiloride as amiloride-sensitive PD.

Statistical analysis

Results are presented as mean \pm SEM. Throughout the study, and if not otherwise stated, data were analyzed by one-way ANOVA. Unpaired *t* test was used for the comparison between 2 groups (Fig. 7B). $P < 0.05$ was considered statistically significant.

Acknowledgements

We thank Anne-Marie Mérillat for excellent photographic work and Friedrich Beermann for critically reading the manuscript. We are grateful to Jean-Christophe Stehle and Samuel Rotman from the mouse histology platform of the University of Lausanne. This work was supported by grants from the Swiss National Science Foundation and the National Center of Competence in Research NCCR: Kidney.CH: Control of homeostasis and the Leducq Foundation to EH. SM was a recipient of the FBM fellowship program of the University of Lausanne, Switzerland. Part of this work has been published in abstract form ^{44,45}.

Statement of competing financial interests

None

References:

1. Staub, O, Loffing, J: Chapter 35 - Mineralocorticoid Action in the Aldosterone Sensitive Distal Nephron. In: *Seldin and Giebisch's The Kidney (Fifth Edition)*. Academic Press, 2013, pp 1181-1211.
2. Zennaro, MC, Jeunemaitre, X, Boulkroun, S: Integrating genetics and genomics in primary aldosteronism. *Hypertension*, 60: 580-588, 2012.
3. Lifton, RP: Genetic diseases of the kidney. Amsterdam; Boston, Elsevier/Academic Press, 2009.
4. Canessa, CM, Horisberger, JD, Rossier, BC: Epithelial sodium channel related to proteins involved in neurodegeneration. *Nature*, 361: 467-470, 1993.
5. Canessa, CM, Schild, L, Buell, G, Thorens, B, Gautschi, I, Horisberger, JD, Rossier, BC: Amiloride-sensitive epithelial Na⁺ channel is made of three homologous subunits. *Nature*, 367: 463-467, 1994.
6. Hummler, E, Barker, P, Gatzky, J, Beermann, F, Verdumo, C, Schmidt, A, Boucher, R, Rossier, BC: Early death due to defective neonatal lung liquid clearance in alpha-ENaC-deficient mice. *Nat Genet*, 12: 325-328, 1996.
7. Barker, PM, Nguyen, MS, Gatzky, JT, Grubb, B, Norman, H, Hummler, E, Rossier, B, Boucher, RC, Koller, B: Role of gammaENaC subunit in lung liquid clearance and electrolyte balance in newborn mice. Insights into perinatal adaptation and pseudohypoaldosteronism. *The Journal of clinical investigation*, 102: 1634-1640, 1998.
8. McDonald, FJ, Yang, B, Hrstka, RF, Drummond, HA, Tarr, DE, McCray, PB, Jr., Stokes, JB, Welsh, MJ, Williamson, RA: Disruption of the beta subunit of the epithelial Na⁺ channel in mice: hyperkalemia and neonatal death associated with a

- pseudohypoaldosteronism phenotype. *Proc Natl Acad Sci U S A*, 96: 1727-1731, 1999.
9. Rubera, I, Loffing, J, Palmer, LG, Frindt, G, Fowler-Jaeger, N, Sauter, D, Carroll, T, McMahon, A, Hummler, E, Rossier, BC: Collecting duct-specific gene inactivation of alphaENaC in the mouse kidney does not impair sodium and potassium balance. *The Journal of clinical investigation*, 112: 554-565, 2003.
 10. Duc, C, Farman, N, Canessa, CM, Bonvalet, JP, Rossier, BC: Cell-specific expression of epithelial sodium channel alpha, beta, and gamma subunits in aldosterone-responsive epithelia from the rat: localization by in situ hybridization and immunocytochemistry. *J Cell Biol*, 127: 1907-1921, 1994.
 11. Kunzelmann, K, Mall, M: Electrolyte transport in the mammalian colon: mechanisms and implications for disease. *Physiological reviews*, 82: 245-289, 2002.
 12. Koyama, K, Sasaki, I, Naito, H, Funayama, Y, Fukushima, K, Unno, M, Matsuno, S, Hayashi, H, Suzuki, Y: Induction of epithelial Na⁺ channel in rat ileum after proctocolectomy. *Am J Physiol-Gastr L*, 276: G975-G984, 1999.
 13. Lingueglia, E, Renard, S, Waldmann, R, Voilley, N, Champigny, G, Plass, H, Lazdunski, M, Barbry, P: Different homologous subunits of the amiloride-sensitive Na⁺ channel are differently regulated by aldosterone. *J Biol Chem*, 269: 13736-13739, 1994.
 14. Renard, S, Voilley, N, Bassilana, F, Lazdunski, M, Barbry, P: Localization and regulation by steroids of the alpha, beta and gamma subunits of the amiloride-sensitive Na⁺ channel in colon, lung and kidney. *Pflugers Arch*, 430: 299-307, 1995.
 15. Asher, C, Wald, H, Rossier, BC, Garty, H: Aldosterone-induced increase in the abundance of Na⁺ channel subunits. *Am J Physiol*, 271: C605-611, 1996.
 16. Sandle, GI: Salt and water absorption in the human colon: a modern appraisal. *Gut*, 43: 294-299, 1998.

17. Pradervand, S, Wang, Q, Burnier, M, Beermann, F, Horisberger, JD, Hummler, E, Rossier, BC: A mouse model for Liddle's syndrome. *J Am Soc Nephrol*, 10: 2527-2533, 1999.
18. Pradervand, S, Vandewalle, A, Bens, M, Gautschi, I, Loffing, J, Hummler, E, Schild, L, Rossier, BC: Dysfunction of the epithelial sodium channel expressed in the kidney of a mouse model for Liddle syndrome. *J Am Soc Nephrol*, 14: 2219-2228, 2003.
19. Bertog, M, Cuffe, JE, Pradervand, S, Hummler, E, Hartner, A, Porst, M, Hilgers, KF, Rossier, BC, Korbmayer, C: Aldosterone responsiveness of the epithelial sodium channel (ENaC) in colon is increased in a mouse model for Liddle's syndrome. *J Physiol*, 586: 459-475, 2008.
20. Amasheh, S, Barmeyer, C, Koch, CS, Tavalali, S, Mankertz, J, Epple, HJ, Gehring, MM, Florian, P, Kroesen, AJ, Zeitz, M, Fromm, M, Schulzke, JD: Cytokine-dependent transcriptional down-regulation of epithelial sodium channel in ulcerative colitis. *Gastroenterology*, 126: 1711-1720, 2004.
21. Zeissig, S, Bergann, T, Fromm, A, Bojarski, C, Heller, F, Guenther, U, Zeitz, M, Fromm, M, Schulzke, JD: Altered ENaC expression leads to impaired sodium absorption in the noninflamed intestine in Crohn's disease. *Gastroenterology*, 134: 1436-1447, 2008.
22. Vallet, V, Chraibi, A, Gaeggeler, HP, Horisberger, JD, Rossier, BC: An epithelial serine protease activates the amiloride-sensitive sodium channel. *Nature*, 389: 607-610, 1997.
23. Vuagniaux, G, Vallet, V, Jaeger, NF, Hummler, E, Rossier, BC: Synergistic activation of ENaC by three membrane-bound channel-activating serine proteases (mCAP1, mCAP2, and mCAP3) and serum- and glucocorticoid-regulated kinase (Sgk1) in *Xenopus* Oocytes. *J Gen Physiol*, 120: 191-201, 2002.

24. Vuagniaux, G, Vallet, V, Jaeger, NF, Pfister, C, Bens, M, Farman, N, Courtois-Coutry, N, Vandewalle, A, Rossier, BC, Hummler, E: Activation of the amiloride-sensitive epithelial sodium channel by the serine protease mCAP1 expressed in a mouse cortical collecting duct cell line. *J Am Soc Nephrol*, 11: 828-834, 2000.
25. Adachi, M, Kitamura, K, Miyoshi, T, Narikiyo, T, Iwashita, K, Shiraishi, N, Nonoguchi, H, Tomita, K: Activation of epithelial sodium channels by prostaticin in *Xenopus* oocytes. *J Am Soc Nephrol*, 12: 1114-1121, 2001.
26. Planes, C, Randrianarison, NH, Charles, RP, Frateschi, S, Cluzeaud, F, Vuagniaux, G, Soler, P, Clerici, C, Rossier, BC, Hummler, E: ENaC-mediated alveolar fluid clearance and lung fluid balance depend on the channel-activating protease 1. *EMBO Mol Med*, 2: 26-37, 2010.
27. Wang, Q, Horisberger, JD, Maillard, M, Brunner, HR, Rossier, BC, Burnier, M: Salt- and angiotensin II-dependent variations in amiloride-sensitive rectal potential difference in mice. *Clin Exp Pharmacol Physiol*, 27: 60-66, 2000.
28. Wang, H, Garvin, JL, Carretero, OA: Angiotensin II enhances tubuloglomerular feedback via luminal AT(1) receptors on the macula densa. *Kidney international*, 60: 1851-1857, 2001.
29. Pradervand, S, Barker, PM, Wang, Q, Ernst, SA, Beermann, F, Grubb, BR, Burnier, M, Schmidt, A, Bindels, RJ, Gatzky, JT, Rossier, BC, Hummler, E: Salt restriction induces pseudohypoaldosteronism type 1 in mice expressing low levels of the beta-subunit of the amiloride-sensitive epithelial sodium channel. *Proc Natl Acad Sci U S A*, 96: 1732-1737, 1999.
30. Machnik, A, Neuhofer, W, Jantsch, J, Dahlmann, A, Tammela, T, Machura, K, Park, JK, Beck, FX, Muller, DN, Derer, W, Goss, J, Ziomber, A, Dietsch, P, Wagner, H, van Rooijen, N, Kurtz, A, Hilgers, KF, Alitalo, K, Eckardt, KU, Luft, FC, Kerjaschki, D,

- Titze, J: Macrophages regulate salt-dependent volume and blood pressure by a vascular endothelial growth factor-C-dependent buffering mechanism. *Nature medicine*, 15: 545-552, 2009.
31. Sorensen, MV, Matos, JE, Praetorius, HA, Leipziger, J: Colonic potassium handling. *Pflugers Arch*, 459: 645-656, 2010.
32. Frateschi, S, Keppner, A, Malsure, S, Iwaszkiewicz, J, Sergi, C, Merillat, AM, Fowler-Jaeger, N, Randrianarison, N, Planes, C, Hummler, E: Mutations of the Serine Protease CAP1/Prss8 Lead to Reduced Embryonic Viability, Skin Defects, and Decreased ENaC Activity. *Am J Pathol*, 181: 605-615, 2012.
33. Hummler, E, Dousse, A, Rieder, A, Stehle, JC, Rubera, I, Osterheld, MC, Beermann, F, Frateschi, S, Charles, RP: The channel-activating protease CAP1/Prss8 is required for placental labyrinth maturation. *PloS one*, 8: e55796, 2013.
34. Leyvraz, C, Charles, RP, Rubera, I, Guitard, M, Rotman, S, Breiden, B, Sandhoff, K, Hummler, E: The epidermal barrier function is dependent on the serine protease CAP1/Prss8. *J Cell Biol*, 170: 487-496, 2005.
35. Frateschi, S, Camerer, E, Crisante, G, Rieser, S, Membrez, M, Charles, RP, Beermann, F, Stehle, JC, Breiden, B, Sandhoff, K, Rotman, S, Haftek, M, Wilson, A, Ryser, S, Steinhoff, M, Coughlin, SR, Hummler, E: PAR2 absence completely rescues inflammation and ichthyosis caused by altered CAP1/Prss8 expression in mouse skin. *Nature communications*, 2: 161, 2011.
36. Hummler, E, Merillat, AM, Rubera, I, Rossier, BC, Beermann, F: Conditional gene targeting of the Scnn1a (alphaENaC) gene locus. *Genesis*, 32: 169-172, 2002.
37. Rubera, I, Meier, E, Vuagniaux, G, Merillat, AM, Beermann, F, Rossier, BC, Hummler, E: A conditional allele at the mouse channel activating protease 1 (Prss8) gene locus. *Genesis*, 32: 173-176, 2002.

38. Sorensen, MV, Grossmann, S, Roesinger, M, Gresko, N, Todkar, AP, Barmettler, G, Ziegler, U, Odermatt, A, Loffing-Cueni, D, Loffing, J: Rapid dephosphorylation of the renal sodium chloride cotransporter in response to oral potassium intake in mice. *Kidney international*, 83: 811-824, 2013.
39. Wagner, CA, Loffing-Cueni, D, Yan, Q, Schulz, N, Fakitsas, P, Carrel, M, Wang, T, Verrey, F, Geibel, JP, Giebisch, G, Hebert, SC, Loffing, J: Mouse model of type II Bartter's syndrome. II. Altered expression of renal sodium- and water-transporting proteins. *Am J Physiol Renal Physiol*, 294: F1373-1380, 2008.
40. Planes, C, Leyvraz, C, Uchida, T, Angelova, MA, Vuagniaux, G, Hummler, E, Matthay, M, Clerici, C, Rossier, B: In vitro and in vivo regulation of transepithelial lung alveolar sodium transport by serine proteases. *Am J Physiol Lung Cell Mol Physiol*, 288: L1099-1109, 2005.
41. Meneton, P, Schultheis, PJ, Greeb, J, Nieman, ML, Liu, LH, Clarke, LL, Duffy, JJ, Doetschman, T, Lorenz, JN, Shull, GE: Increased sensitivity to K⁺ deprivation in colonic H,K-ATPase-deficient mice. *The Journal of clinical investigation*, 101: 536-542, 1998.
42. List, K, Kosa, P, Szabo, R, Bey, AL, Wang, CB, Molinolo, A, Bugge, TH: Epithelial integrity is maintained by a matriptase-dependent proteolytic pathway. *Am J Pathol*, 175: 1453-1463, 2009.
43. Christensen, BM, Perrier, R, Wang, Q, Zuber, AM, Maillard, M, Mordasini, D, Malsure, S, Ronzaud, C, Stehle, JC, Rossier, BC, Hummler, E: Sodium and potassium balance depends on alphaENaC expression in connecting tubule. *J Am Soc Nephrol*, 21: 1942-1951, 2010.

44. Malsure, S, Charles, R-P, Wang Q, Christensen, B, Perrier, R, Rossier, B, Hummler E: Implication of ENaC and its positive regulator CAP1/Prss8 in whole net sodium homeostasis. *J Am Soc Nephrol (Suppl)* 2009; 14A.
45. Malsure, S, Perrier, M, Maillard, M, Rossier, BC, Hummler, E: Colon specific α ENaC gene inactivation fully inhibits electrogenic amiloride sensitive sodium transport, leading to sodium loss in faeces without compromising overall sodium and potassium balance. *J Am Soc Nephrol (Suppl)* 2012; 496A.

Figure legends

Figure 1. Generation of colonic superficial cell-specific *Scnn1a*-deficient mice.

DNA, mRNA and proteins samples were analyzed from tissues (A) or isolated distal colonic superficial cells (A-D). (A) PCR analysis on ear biopsies with primers distinguishes between the lox (580 bp) and the KO (360 bp) allele of the *Scnn1a* gene locus (top). In the middle, primers indicated distinguish between wt (+; 220 bp), and lox (280 bp) allele in experimental *Scnn1a*^{lox/-};villin::Cre^{tg/+} (*Scnn1a*^{KO}) and controls, lane 1-2, *Scnn1a*^{lox/-} (*Scnn1a*^{Het}); lane 3-4, *Scnn1a*^{lox/+};villin::Cre^{tg/+} (*Scnn1a*^{Hetc}); lane 5-6, and *Scnn1a*^{lox/+} (*Scnn1a*^{Lox}); lane 7-8 littermates. Detection of the *villin::Cre* transgene using Cre-specific primers. Myogenin-specific primers were used as internal control (lower panel). (B) Quantification of α , β , γ ENaC mRNA transcripts by qRT-PCR in distal colonic scrapped cells from *Scnn1a*^{Lox} (n=5, white), *Scnn1a*^{Het} (n=4, light grey) and *Scnn1a*^{KO} mice (n=4, black column). Results are expressed as the ratio of mRNA/ β -actin mRNA (*, $P < 0.05$). (C) Representative immunoblot showing the expression of α ENaC and β -actin protein in scraped distal colon cells from *Scnn1a*^{Lox}, *Scnn1a*^{Het}, *Scnn1a*^{Hetc} and *Scnn1a*^{KO} mice. (D) Quantification of α ENaC protein expression levels in scraped distal colon cells from *Scnn1a*^{Lox} (white), *Scnn1a*^{Het} (light grey), *Scnn1a*^{Hetc} (dark grey) and *Scnn1a*^{KO} (black) mice after analysis with ImageJ software; (n=3 mice per group, *, $P < 0.05$). Results are expressed as the ratio of α ENaC protein/ β -actin protein. Values are mean \pm S.E.M.

Figure 2. Colonic sodium transport was affected in *Scnn1a*^{KO} mice

Morning and afternoon measurements of amiloride-sensitive rectal potential difference (Δ PD_{amil}, mV) on 2 consecutive days in *Scnn1a*^{Lox} mice (n= 7; —), *Scnn1a*^{Het} (n=7; ---), *Scnn1a*^{Hetc} (n=7 ; ···) and *Scnn1a*^{KO}, (n=8 ; ·-·-·) mice treated with high (HS, A), regular (RS, B), or low salt (LS, C) diets. ***, $P < 0.001$. Values are mean \pm S.E.M.

Figure 3. *Scnn1a*^{KO} mice showed elevated plasma aldosterone levels

Plasma aldosterone (nmol/l) concentrations in *Scnn1a*^{Lox} (n= 6; white), *Scnn1a*^{Het} (n=7; light grey), *Scnn1a*^{Hetc} (n=6 ; dark grey) and *Scnn1a*^{KO} (n= 7; black) mice groups were analysed upon various sodium diets. *, $P < 0.05$; **, $P < 0.01$; RS, regular salt; LS, low salt and HS, High salt diet. Values are mean \pm S.E.M.

Figure 4. Sodium is lost through feces in *Scnn1a*^{KO} mice

Measurements of sodium (mmol/24h, **A**) and potassium (mmol/24h, **B**) electrolytes levels in feces from *Scnn1a*^{Lox} (n=6; white), *Scnn1a*^{Het} (n=7; light grey) and *Scnn1a*^{KO} (n=7 ; black) mice upon various sodium diets. Values are mean \pm S.E.M; *, $P < 0.05$ ***; $P < 0.001$, *Scnn1a*^{KO} vs. *Scnn1a*^{Lox} and *Scnn1a*^{Het} mice.

Figure 5. Diet-dependent sodium loss in urine of *Scnn1a*^{KO} mice

Measurement of cumulative urinary sodium (**A- C**, mmol) and potassium electrolyte (**D-F**, mmol) levels in *Scnn1a*^{Lox} (n=8 ; white), *Scnn1a*^{Het} (n= 7; light grey), *Scnn1a*^{Hetc} (n=8 ; dark grey) and *Scnn1a*^{KO} (n=8 ; black) mice upon High salt (HS; **A**), regular salt (RS; **B**), and low salt (LS; **C**) diets; *, $P < 0.05$; Values are mean \pm S.E.M.

Figure 6. Generation of intestine-specific *Prss8*^{KO} mice

DNA, mRNA and proteins samples were analyzed from isolated intestinal superficial cells as indicated (**A-D**). (**A**) DNA-based PCR analysis on ear biopsies using primers distinguishing wild-type (+; 379 bp), lox (413 bp) and Δ allele (top, 473 bp) in *Prss8*^{lox/+} (*Prss8*^{Lox}, lane 1-4), *Prss8*^{lox/ Δ} (*Prss8*^{Het}, lane 5-8) and *Prss8* ^{Δ /lox}; *villin::Cre*^{tg/+} (*Prss8*^{KO}; lane 9-12) littermates. The *villin::Cre* transgene (bottom, 400 bp) and myogenin (internal control) are detected using

specific primers. **(B)** Quantification of *CAP1/Prss8*, *CAP2/Tmprss4* and *CAP3/SP14* mRNA transcripts by qRT-PCR in pooled scraped colon cells from *Prss8^{Lox}* (n=4, white), *Prss8^{Het}* (n=5, grey) and *Prss8^{KO}* (n=8, black) mice. Data are expressed as the ratio of mRNA/ β -actin mRNA. *: $P < 0.05$). **(C)** Representative immunoblot showing the expression of *CAP1/Prss8* and β -actin protein in scraped colon cells from *Prss8^{Lox}*, *Prss8^{Het}* and knockouts *Prss8^{KO}*. **(D)** Quantification of *CAP1/Prss8* signals in *Prss8^{Lox}* (n=4, white), *Prss8^{Het}* (n=5, grey) and *Prss8^{KO}* (n=6, black) scraped colon cells analyzed with ImageJ software; (***, $P < 0.001$). Results are expressed as the ratio of *CAP1/Prss8* protein/ β -actin protein. Values are mean \pm S.E.M.

Figure 7. CAP1/Prss8 is as a regulator of ENaC in colon

(A) Morning and afternoon measurements of amiloride-sensitive rectal potential difference (ΔPD_{amil} , mV) on 2 consecutive days in control (*Prss8^{Lox}* (n= 8; —), *Prss8^{Het}* (n=7; ---) and *Prss8^{KO}* (n= 8; ---) mice treated with High salt (HS, **A**), regular salt (RS, **B**), and low salt (LS, **C**) diet. **(D)** Plasma aldosterone concentrations following various sodium diets (nmol/l). **(E)** Fecal sodium and **(F)** fecal potassium concentrations (mmol/24h) in *Prss8^{Lox}* (n=5; white), *Prss8^{Het}* (n= 6; grey) and *Prss8^{KO}* (n=6; black) mice following a high-salt (HS), a regular-salt (RS) and low salt (LS) diet; *, $P < 0.05$. Values are mean \pm S.E.M.

Figure 8. Shifted sodium balance under HS, RS and LS diets in *Scnn1a^{KO}* mice

Sodium balance is considered as ratio between the quantity of sodium output (in urine or in feces) at day 1 normalized by the quantity of sodium intake at day 1. Data were taken from experiments summarized in **Table 1** (food intake), **Fig. 4** (fecal sodium) and **Fig. 5** (urinary sodium). For each of the genotypes (*Scnn1a^{Lox}*, *Scnn1a^{Het}* and *Scnn1a^{KO}*) the average sodium intake via food (grey column) is compared with urinary sodium-output (white

column) and fecal sodium output (black column) upon high (HS), regular (RS) or low (LS) salt diet.

Table 1: Physiological parameters of *Scnn1a*^{KO} mice

Physiological parameters in *Scnn1a*^{Lox}, *Scnn1a*^{Het} and *Scnn1a*^{KO} mice following different diets. Data are mean ± SEM.

Parameters	Regular salt diet			Low salt diet		
	<i>Scnn1a</i> ^{Lox}	<i>Scnn1a</i> ^{Het}	<i>Scnn1a</i> ^{KO}	<i>Scnn1a</i> ^{Lox}	<i>Scnn1a</i> ^{Het}	<i>Scnn1a</i> ^{KO}
n	7	5	9	5	5	4
BW(g)	25.83±1.5	25.92±0.4	26.75±1	25.50±1.2	24.80±0.2	23.83±0.7
Food intake/body weight ratio	0.13±0.02	0.15±0.0	0.14±0.03	0.12±0.01	0.13±0.0	0.13±0.0
Water intake/body weight ratio	0.16±0.01	0.16±0.03	0.22±0.02	0.16±0.04	0.18±0.01	0.22±0.02
Urine output /body weight ratio	0.05±0.01	0.06±0.01	0.08±0.01	0.06±0.02	0.05±0.01	0.06±0.06
Feces output/body weight ratio	0.02±0.0	0.02±0.01	0.02±0.0	0.02±0.0	0.02±0.0	0.02±0.0
Plasma Na ⁺ (mM)	151.6±1.2	149±0.2	161±4.2	148.2±2.2	153±2.4	148±1.07
Plasma K ⁺ (mM)	5.2±0.2	4.28±0.2	5.1±0.28	4.23±0.2	4.62±0.2	4.83±0.07
	High salt diet			High potassium diet (48 hrs)		
n	4	4	4	4	4	4
BW(g)	25.83±0.6	25.41±0.5	25.13±0.4	26.34±0.3	25.21±0.2	25.23±0.2
Food intake/body weight ratio	0.11±0.02	0.12±0.02	0.11±0.0	0.11±0.03	0.10±0.01	0.11±0.01
Water intake/body weight ratio	0.19±0.01	0.20±0.10	0.21±0.01	0.12±0.03	0.11±0.01	0.12±0.01
Urine output /body weight ratio	1.6±0.01	1.7±0.01	1.75±0.02	0.04±0.03	0.05±0.01	0.04±0.01
Feces output/body weight ratio	0.01±0.0	0.01±0.0	0.01±0.0	0.01±0.0	0.01±0.0	0.01±0.0
Plasma Na ⁺ (mM)	154±1.2	152±0.2	157±4.3	159.8±3.1	162±4.2	159.7±2.1
Plasma K ⁺ (mM)	5.1±0.29	4.5±0.2	5.1±0.2	4.3±0.1	4.1±0.5	4.4±0.5
Urinary Na ⁺ (mM/24h)				0.39±0.03	0.34±0.1	0.37±0.1
Urinary K ⁺ (mM/24h)				3.6±1	3.1±1.1	3.6±1.2

Table 2: Physiological parameters of *Prss8*^{KO} mice

Physiological parameters in *Prss8*^{Lox}, *Prss8*^{Het} and *Prss8*^{KO} mice following different diets.

Data are mean ± SEM.

Parameters	Regular salt diet			Low salt diet		
	<i>Prss8</i> ^{Lox}	<i>Prss8</i> ^{Het}	<i>Prss8</i> ^{KO}	<i>Prss8</i> ^{Lox}	<i>Prss8</i> ^{Het}	<i>Prss8</i> ^{KO}
n	7	5	9	5	5	4
BW (g)	24.95±0.6	24.12±0.3	25.15±0.4	23.93±0.8	22.30±0.2	22.15±0.4
Food intake/body weight ratio	0.12±0.3	0.13±0.3	0.12±0.9	0.12±0.2	0.13±0.3	0.12±0.3
Water intake/body weight ratio	0.15±0.1	0.15±0.3	0.16±0.2	0.16±0.1	0.16±0.1	0.18±0.1
Urine output /body weight ratio	0.04±1.1	0.05±0.4	0.05±0.3	0.05±0.1	0.05±0.1	0.06±0.3
Feces output/body weight ratio	0.02±0.2	0.01±0.0	0.01±0.0	0.02±0.0	0.01±0.0	0.02±0.0
Plasma Na⁺(mM)	154±4.3	155±1.5	152±2.9	138±1.5	142±1.2	135±3.8
Plasma K⁺(mM)	4.5±0.1	4.7±0.09	4.8±0.1	4.6±0.2	4.3±0.5	4.4±0.1
Urinary Na⁺(mM)	37±1.9	24±1.3	25±8.2	6.6±1.0	6.39±0.34	8.3±0.48
Urinary K⁺(mM)	35±1.8	30.2±2.3	30.19±2.4	59±8.1	58±3.23	62±3.05
	High salt diet					
n	4	4	4			
BW (g)	21.30±0.6	21.45±0.4	20.12±0.3			
Food intake/body weight ratio	0.12±0.2	0.12±0.2	0.11±0.3			
Water intake/body weight ratio	0.17±0.1	0.18±0.1	0.19±0.1			
Urine output /body weight ratio	1.8±0.1	1.8±0.1	1.85±0.3			
Feces output/body weight ratio	0.01±0.0	0.02±0.0	0.01±0.0			
Plasma Na⁺(mM)	147±1.8	143±1.02	142±1.02			
Plasma K⁺(mM)	5±0.1	4.8±0.2	5.08±0.1			
Urinary Na⁺(mM)	163±10.2	168±14.56	186±11.7			
Urinary K⁺(mM)	25.5±3.1	26.34±4.1	26.44±2.8			

Figure 1

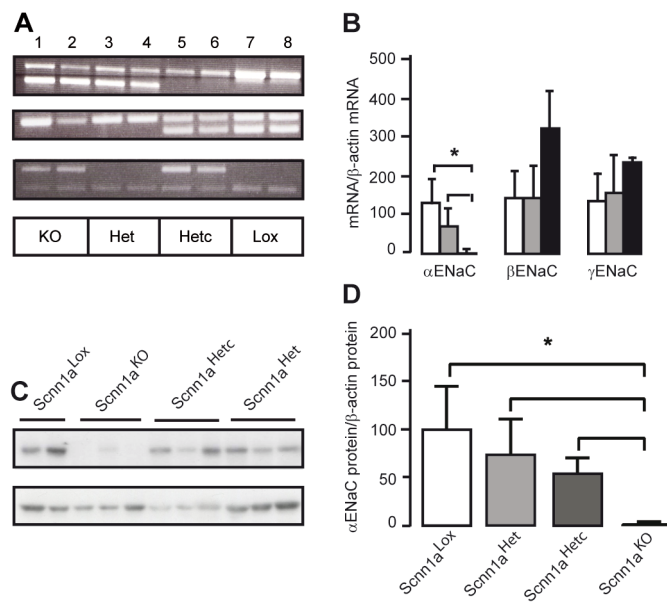


Figure 2

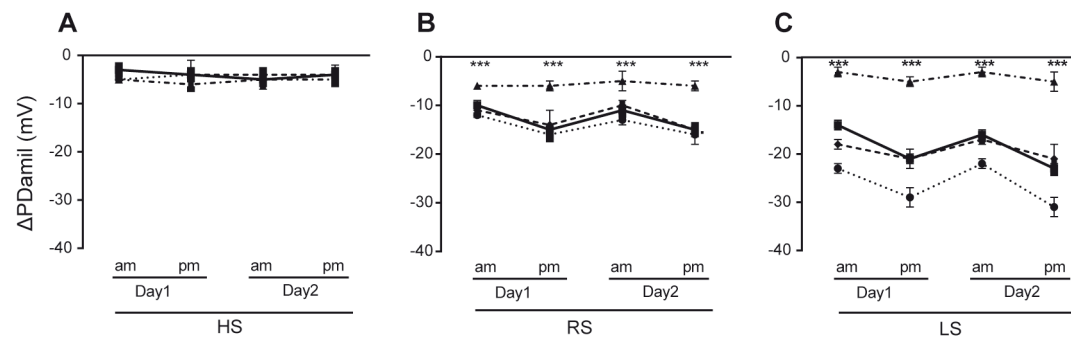


Figure 3

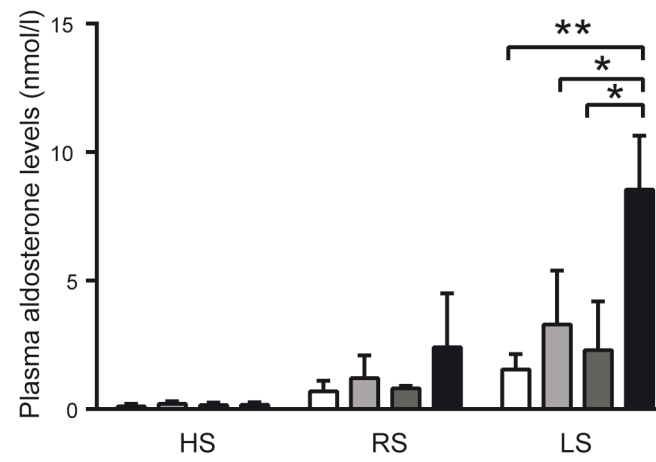


Figure 4

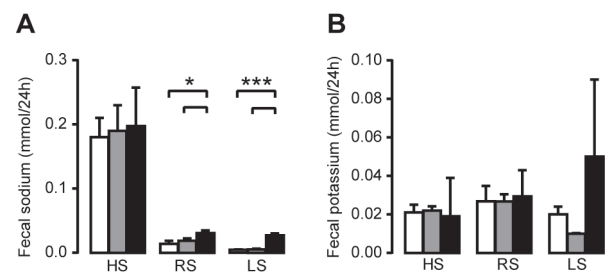


Figure 5

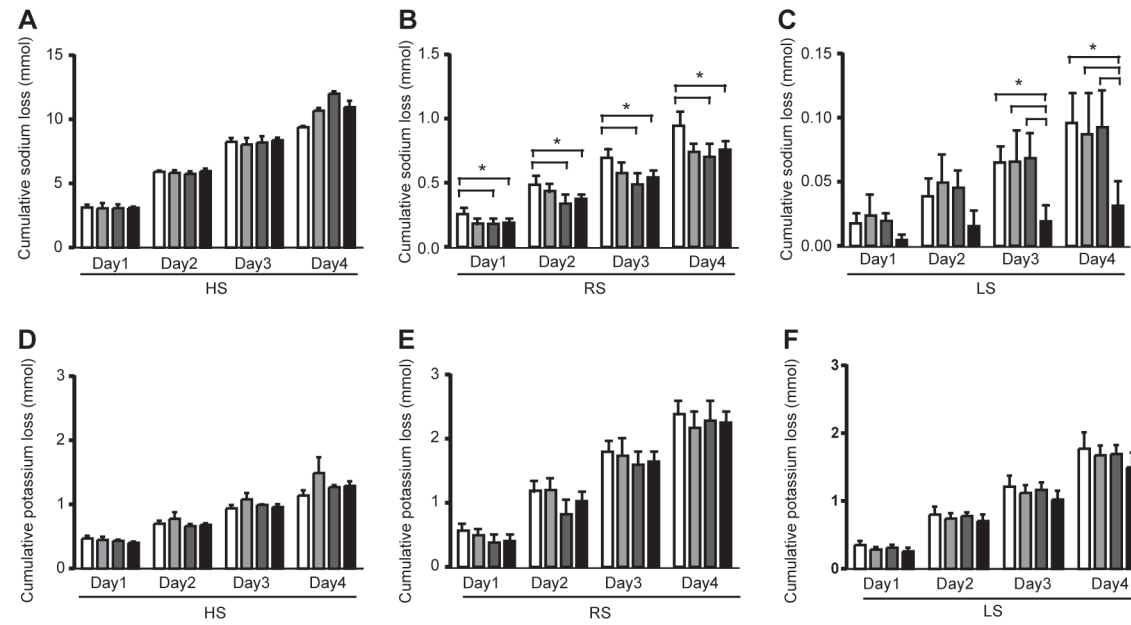


Figure 6

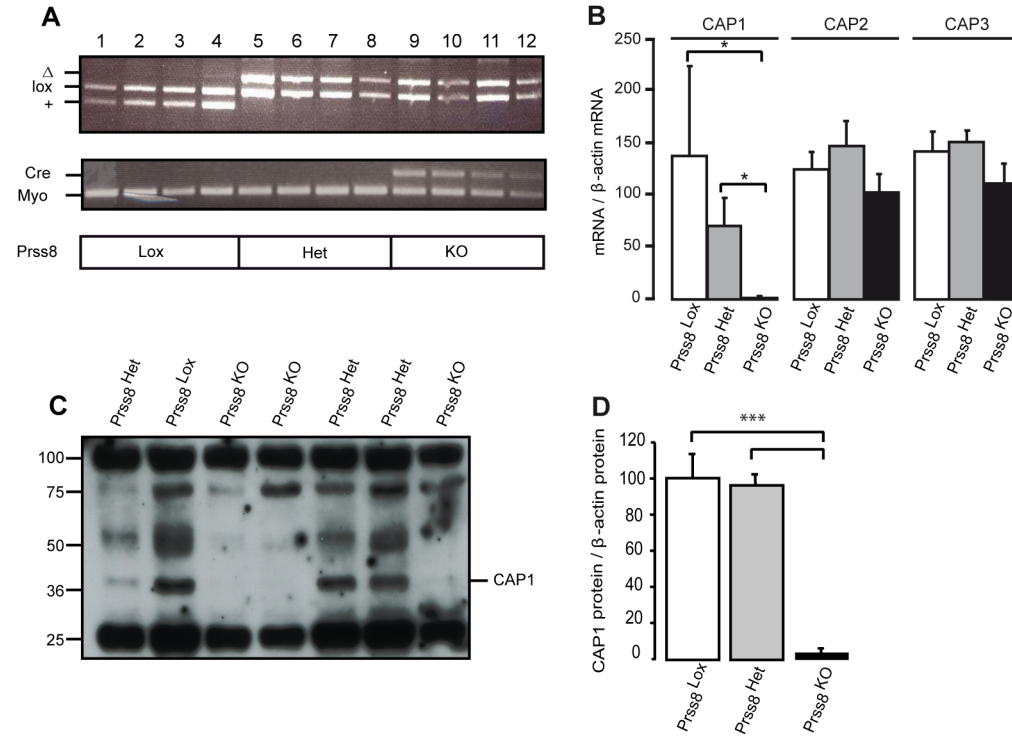


Figure 7

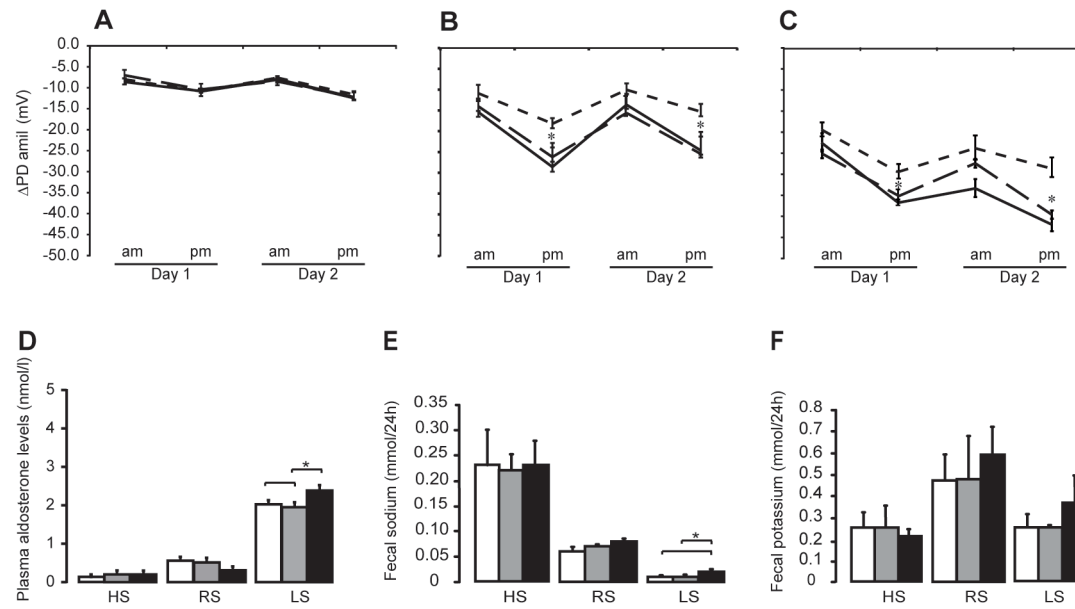


Figure 8

